Alfvèn waves within the Earth's core

D. Jault, and G. Légaut

LGIT, CNRS, Université Joseph Fourier, BP 53, F-38041 Grenoble Cedex 9, France

Abstract

Alfvén waves within the Earth's fluid core have been detected through the monitoring of the magnetic field at observatories situated on the Earth's surface. Inside the core, geostrophic motions consist of oscillations of cylindrical annuli about the rotation axis and propagate as Alfvèn waves, with periods in the range 10-100 years. These waves cause torques acting on the mantle and yield time changes of the rotation period of the solid Earth that are also monitored. From a modeling of these waves, Zatman and Bloxham had initiated the inversion of the magnetic field threading the coaxial geostrophic cylinders in the core interior.

We give an account of existing theoretical models of torsional Alfvèn waves within the Earth's core. We complement the previous studies that have considered standing waves only by investigating the propagation of torsional Alfvèn waves as an initial value problem instead. Interestingly, the direction of propagation of the waves may indicate where dissipation takes place. In this respect, including a solid inner core in the model is crucial.

1 Introduction

The Coriolis force is a key ingredient of large scale dynamics of the Earth's fluid core, where the waves that are the more important in the dynamo process and have periods on the order of the magnetic diffusion time are strongly influenced by rotation. An exact balance between the Coriolis and pressure forces set apart the geostrophic motions, which are readily accelerated by Lorentz and other forces. They can form fast Alfvèn waves, weakly influenced by magnetic diffusion. These transverse waves propagate in the directions perpendicular to the rotation axis. Their frequency is linearly dependent on the intensity of the magnetic field transverse to the wave motions [Roberts, 1967]. Their study, which was initiated by Braginsky [1970], has thus the potential to give precious informations on the otherwise hidden magnetic field within the core [Zatman and Bloxham, 1998].

Models of the magnetic field at the Earth's surface can be downward continued to the surface of the metallic core because the solid mantle of the Earth is almost electrically insulating. At the Earth's surface, the declination of the magnetic field has been mapped for a few centuries [Jonkers et al., 2003]. It turns out that this is the appropriate timescale to study the evolution of the large scale (up to harmonic degree 3-4) and nondipolar parts of the magnetic field. Measurements at magnetic observatories have enabled to characterize changes in the Earth magnetic field up to degree 6-8 for the last century. Finally, variations of the magnetic field up to degree 13 between 1980 and 2000 [Hulot et al., 2002] and up to degree 11 during the last few years [Olsen, 2002] have been recently retrieved from satellite measurements. We note that the variation of the magnetic field of harmonic degree 13 between 1980 and 2000 at the Earth's surface is comparable but still smaller to the total intensity of the magnetic field of this degree at either of the two epochs [Hulot et al., 2002]. It is now well established that the duration of magnetic field features is decreased in proportion of their lengthscale, as expected from a physical standpoint. Unfortunately, the rapid attenuation of small scale features of the Earth's magnetic field throughout the mantle will severely limit our ability to map it at the CMB.

In addition to these variations, sudden changes of the large scale part of the magnetic field have been detected in observatories. They occur simultaneously throughout large regions of the Earth's surface [Alexandrescu et al., 1996]. These events can be characterized as very rapid changes of the rate of variation of the Earth's magnetic field. It is customary to call them "jerks". The first global one to be detected occurred in 1969. It has been followed by similar events in 1978, 1991 and 1999. Their recurrence period is reminiscent of the solar cycle. However, the magnetic signal has predominantly an internal origin according to spherical harmonic analyses [Malin and Hodder, 1982] and the magnetic jerks were first detected after isolation of the solar-cycle related variation [Ducruix et al., 1980]. With one exception [Duhau and Martinez, 1995], studies of the internal part of the solar-cycle related variation have considered only magnetic induction in the solid mantle, leaving out processes in the liquid core. Bloxham et al. [2002] have just argued that the regularity of the occurrence of jerks during the last thirty years may result from the propagation of Alfvèn torsional waves within the Earth's core.

It is only recently that a host of geophysical applications followed up the initial study of Braginsky [1970]. The trace of Alfvèn waves has been searched in models of core surface flow $\mathbf{u}$, of typical speed a few $10^{-4} m.s^{-1}$, derived from the secular variation (SV) of the Earth's magnetic field through the equation:

$$\frac{\partial B_r}{\partial t} = -\boldsymbol{\nabla}_H \cdot (\mathbf{u} B_r) , \tag{1}$$

where B_r is the radial component of the magnetic field at the core-mantle boundary (CMB), inferred from models of the magnetic field at the Earth's surface, assuming an insulating mantle. This approach has been validated when it has been shown that changes in core angular momentum carried by geostrophic motions extracted from surface flow models balance fairly well observed changes in the angular momentum of the solid Earth [Jault et al., 1988, Jackson et al., 1993, Hide et al., 2000, Pais and Hulot, 2000]. The basic tenet of these studies is that time-dependent zonal motions are geostrophic. The main difficulty is that zonal motions are not dominant at the core surface. It is compounded by the lack of models accounting for the non-zonal part of the motions. Recent maps of flow at the core surface show strong westward winds in the equatorial region of the Atlantic hemisphere and few motions in the Pacific hemisphere. After these early studies, Zatman and Bloxham [1997] noted that most of the zonal motions $u_\phi(\theta)$ (u_ϕ orthoradial component, θ colatitude) symmetrical about the equator of their velocity models from 1900 to 1990 can be fitted as the sum of two standing oscillations, with periods 76 and 53 years. Redoing the same analysis for the shorter epoch 1957-2001 with data better resolved in time, Bloxham et al. [2002] found three oscillatory motions, with periods 45, 20 and 13 years.

In the case of axisymmetrical solid boundaries, the torsional Alfvèn equation amounts to an equation for the density of angular momentum within the core. Hide et al. [2000] argued, from the velocity models of Jackson et al. [1993], that there is propagation of core angular momentum density from the equatorial to polar regions. Equations of Alfvèn waves, in an unbounded fluid, are not modified under time inversion. When dissipative terms at the boundaries are omitted, this remains true for the special waves studied here and no direction of propagation is privileged. The observation of Hide et al. [2000], if it is confirmed, thus gives an indication of the importance of dissipation for the evolution of torsional Alfvèn waves inside the core. The question of a favoured direction of propagation has been left untouched by previous models as they were restricted to standing oscillations. In contrast, we choose here to set an initial value problem.

The geometry of the fluid outer core very much dictates the characteristics of these waves. Geostrophic motions $\mathbf{u}_g$ obey the balance:

$$2\rho\left(\mathbf{\Omega}\times\mathbf{u}_g\right) = -\mathbf{\nabla}p_g, \quad \mathbf{u}_g\cdot\mathbf{n}\,|_\Sigma = 0\,, \tag{2}$$

where $\mathbf{n}$ is the outward normal to the boundary Σ of the fluid volume, and p_g the pressure. Geostrophic motions are independent of the coordinate z in the direction of the rotation axis, and are entirely defined by their streamlines on Σ , the pair of geostrophic contours Γ. Denote respectively z_T and z_B the z-coordinates along each upper and lower geostrophic contours. The length $H = z_T - z_B$ is an invariant of each pair of contours and the geostrophic cylinders $\mathcal{C}$ are defined in a unique way by their total height H. The pressure p_g is constant on each cylinder $\mathcal{C}$, parallel to the rotation axis, generated by geostrophic contours. Neither the Coriolis force nor the pressure force enter directly the equation governing the time evolution of the geostrophic velocity. Indeed, integrating the momentum equation on $\mathcal{C}$ to eliminate these forces, as suggested by Bell and Soward [1996], yields:

$$\rho H \oint \left(\frac{\partial \mathbf{u}_g}{\partial t} + \frac{d\Omega}{dt}\mathbf{e}_z\times\mathbf{r}\right).\mathbf{d\Gamma} = \int_0^H \left(\oint_{\Gamma(H,z)} \left(\mathbf{j}\times\mathbf{B}+\rho\mathbf{g}\right).\mathbf{d\Gamma}\right) dz\,, \tag{3}$$

taking into account possible fluctuations of the spin rate Ω of the mantle and noting the position vector $\mathbf{r}$, the unit vector along the rotation axis $\mathbf{e}_z$, the geostrophic contour at the height H above the bottom boundary $\Gamma(H,z)$, the core density ρ, the magnetic field $\mathbf{B}$, the electric current density $\mathbf{j}$, and the buoyancy force $\rho\mathbf{g}$. We omit here both the viscous and the nonlinear terms. Assuming a quasi-static ambient magnetic field, we linearize the expression for the Lorentz force. In presence of the geostrophic motions, a magnetic field $\tilde{\mathbf{b}}$ is induced:

$$\frac{\partial\tilde{\mathbf{b}}}{\partial t} = \nabla \times (\mathbf{u}_g \times \mathbf{B})\,, \tag{4}$$

in the interior of the core, where the time changes of $\tilde{\mathbf{b}}$ are fast enough to make diffusion negligible. Eqs. (3) and (4), with $\tilde{\mathbf{j}} = \nabla\times\tilde{\mathbf{b}}/\mu_0$ and $\mathbf{j}\times\mathbf{B} \simeq \tilde{\mathbf{j}}\times\mathbf{B}+\mathbf{j}\times\tilde{\mathbf{b}}$, are analogous to the equations of Alfvèn waves (μ_0 is the magnetic permeability).

In the case of an axisymmetrical container, the geostrophic contours are circular, the buoyancy term vanishes from Eq. (3), and the magnetic term can be transformed into:

$$\int_{-z_T}^{z_T}\oint (\mathbf{j}\times\mathbf{B})_\phi\, s d\phi dz = \frac{1}{s\mu_0}\frac{\partial}{\partial s}\left(s^2\int_{-z_T}^{z_T}\oint B_s B_\phi d\phi dz\right) \tag{5}$$

$$+\frac{dl}{\mu_0 ds}\left(\oint B_N B_\phi s d\phi\,(z_T) + \oint B_N B_\phi s d\phi\,(-z_T)\right)\,,$$

where (s,ϕ,z) are cylindrical coordinates, dl is the element of length along the boundary in a meridional section, and B_N is the outward normal component of the magnetic field at the boundary. In writing Eq. (5), we have assumed that the container is also symmetrical with respect to the equatorial plane. In the axisymmetrical case, the angular momentum density is constant on each geostrophic cylinder. Multiplying Eq. (3) by the distance s to the rotation axis and integrating it in the fluid volume gives the equation governing the core angular momentum. In this transformation, the first term on the right hand side of (5) vanishes and the last term gives the total electromagnetic torque acting on the core. It vanishes also if the mantle is electrically insulating. Then, there is conservation of the total core angular momentum.

In the next section, we follow the interpretation of the equation of torsional Alfvèn waves within an entirely fluid spherical body in terms of transport of angular momentum. This explains well the amplification of the waves in the vicinity of the equator of the core-mantle boundary (CMB). In the third section, we discuss the influence of possible bumps at the CMB. That enables us to stress that the description in terms of density of angular momentum and torques on geostrophic cylinders is convenient only in the spherical case. We consider also the pressure torque acting on the mantle throughout the propagation of Alfvèn waves. The model is modified to include a solid inner core in a fourth section. At this stage, we have to reinstate the magnetic dissipation also. Finally, we list some works in progress as well as pending problems.

2 Propagation of Alfvèn waves within an entirely fluid spherical body

The study of Alfvèn waves in the spherical case was initiated by Braginsky [1970] from Eqs. (3), (4), and (5). He showed how to eliminate $\tilde{\mathbf{b}}$ except for a surface term. The derivation has just been detailed by Jault [2003]. A magnetic diffusion layer, set up to match the magnetic field induced in the core interior to the magnetic field in the mantle has to be taken into account. In a spherical core, the equation for Alfvèn torsional waves is:

$$
\begin{aligned}
s^3 z_T \frac{\partial^2 (\omega_g + \Omega)}{\partial t^2} &= \frac{1}{\rho\mu_0}\frac{\partial}{\partial s}\left(z_T s^3 \frac{\partial \omega_g}{\partial s}\left\{B_s^2\right\}\right) \\
&- \frac{a s^3}{4\pi\rho z_T}\frac{\partial \omega_g}{\partial t}\oint \left(\sigma_m \Delta B_r^2\right)(z_T) + \left(\sigma_m \Delta B_r^2\right)(-z_T)\, d\phi \\
&+ \frac{a s^2}{4\pi\rho\mu_0 z_T}\oint \left(B_r \frac{\partial \tilde{b}_{m\phi}}{\partial t} + B_\phi \frac{\partial \tilde{b}_{mr}}{\partial t}\right)(z_T) \\
&+ \left(B_r \frac{\partial \tilde{b}_{m\phi}}{\partial t} + B_\phi \frac{\partial \tilde{b}_{mr}}{\partial t}\right)(-z_T)\, d\phi\,, \qquad (6)
\end{aligned}
$$

where (r, θ, ϕ) are spherical coordinates, a the core radius (whence $z_T = (a^2 - s^2)^{1/2}$), $\mathbf{e}_\phi$ the unit azimuthal vector, $\mathbf{u}_g = s\omega_g(s)\mathbf{e}_\phi$, Δ the variable thickness of a hypothetical thin layer of electrical conductivity $\sigma_m(\theta, \phi)$ at the bottom of the mantle, B_r the magnetic field component normal to the core surface, $\tilde{\mathbf{b}}_m$ the magnetic field at the bottom of the insulating volume inside the mantle, and $\left\{B_s^2\right\}$ a measure of the s-component of the magnetic field averaged on each geostrophic cylinder:

$$
\left\{B_s^2\right\}(s) = \frac{1}{4\pi z_T}\int_{-z_T}^{z_T}\oint B_s^2\, d\phi\, dz\,. \qquad (7)
$$

Even though an expression of $\partial\tilde{b}_{mr}/\partial t\,|_{r=a}$ as a function of ω_g is directly obtained from Eq. (4), the determination of $\partial\tilde{b}_{m\phi}/\partial t\,|_{r=a}$ necessitates an integration over the entire core surface. It can be achieved through the calculation of the potential V, such that

$$
\tilde{\mathbf{b}}_m = -\boldsymbol{\nabla} V\,, \qquad (8)
$$

which is derived from $\tilde{b}_{mr}$. In the case of axisymmetrical $\mathbf{B}$ (and thus $\tilde{\mathbf{b}}$), there is no poloidal ingredient in $\tilde{b}_\phi$ and $\tilde{b}_{m\phi}$ vanishes. In the non-axisymmetrical case, however, the last term of Eq. (6) makes the propagation mechanism non local. Time changes of the mantle spin-rate $d\Omega/dt$, which are linearly related to the time changes of core angular momentum carried by geostrophic motions, yield another non-local coupling mechanism between the motions of the different geostrophic cylinders. Indeed, we cannot simply transform Eq. (6) into an equation for $\omega_g^* = (\omega_g + \Omega)$ because of coupling with the mantle (the second term on the right hand side). Eq. (6) is finally completed by two boundary conditions,

$$\frac{\partial \omega_g}{\partial s} = -\mu_0 \left(\oint_{\theta=\pi/2} B_r^2 d\phi \right)^{-1} \left(\oint_{\theta=\pi/2} \sigma_m \Delta B_r^2 d\phi \right) \frac{\partial \omega_g}{\partial t}, \quad \text{at } s = a,$$

which is required to avoid a singularity at $(s = a)$ when $\oint B_r^2 d\phi \neq 0$ at the equator [Buffett, 1998], and

$$\frac{\partial \omega_g}{\partial s} = 0, \quad \text{at } s = 0, \tag{9}$$

in the case of non-axisymmetrical $\mathbf{B}$. The mechanism of propagation is described by the first two terms of Eq. (6). As the wave propagates, there is transport of angular momentum density $z_T s^3 \omega_g$. At the edges of the domain, where either s or z_T vanishes, we expect amplification of ω_g. In the geophysical case, this does not happen near the rotation axis because of the very efficient coupling between the solid and electrically conducting inner core and the wave motions. On the other hand, Fig. 2 of Zatman and Bloxham [1997] indicates amplification of the geostrophic motions at the equator $z_T = 0$. Arguably, their representation minimizes the actual intensification at the equator because of the regularization conditions that are required for the modelling.

We set an initial-value problem. Eq. (6) can be transformed into a set of equations that are readily solved numerically:

$$\begin{aligned} s^3 z_T \frac{\partial (\omega_g + \Omega)}{\partial t} &= \frac{1}{\rho\mu_0} \frac{\partial \tau}{\partial s} \\ &\quad - \frac{a s^3}{4\pi\rho z_T} \left(\oint \sigma_m \Delta B_r^2 d\phi \, (s, z_T) + \oint \sigma_m \Delta B_r^2 d\phi \, (s, -z_T) \right) \omega_g \\ &\quad + \frac{a s^2}{4\pi\rho\mu_0 z_T} \oint \Big[\left(B_r \tilde{b}_{m\phi} + B_\phi \tilde{b}_{mr} \right) (s, z_T) \\ &\quad + \left(B_r \tilde{b}_{m\phi} + B_\phi \tilde{b}_{mr} \right) (s, -z_T) \Big] \, d\phi \,, \qquad (10) \\ \frac{\partial \tau}{\partial t} &= z_T s^3 \frac{\partial \omega_g}{\partial s} \left\{ B_s^2 \right\} \,, \qquad (11) \end{aligned}$$

where τ is an auxiliary variable. This is completed by equations for $\tilde{\mathbf{b}}_m$ at the boundary (see Eq. (8)) and for Ω. As the actual magnetic field in the core interior and the distribution of $\left\{ B_s^2 \right\}$ are unknown, Buffett [1998] based a forward modelling of torsional waves on maps of magnetic field inferred from a numerical geodynamo model. We build a three-dimensional map of the interior magnetic field from models of the large scale magnetic field at the core-mantle boundary, seeking solutions that have the geometry of free decay modes and neglecting entirely the toroidal component. This is acceptable since our calculation has only an illustrative purpose. The root mean square $\left\{ B_s^2 \right\}^{1/2}(s)$, shown on Fig. 1 (full curve), for this ambient magnetic field can be compared with

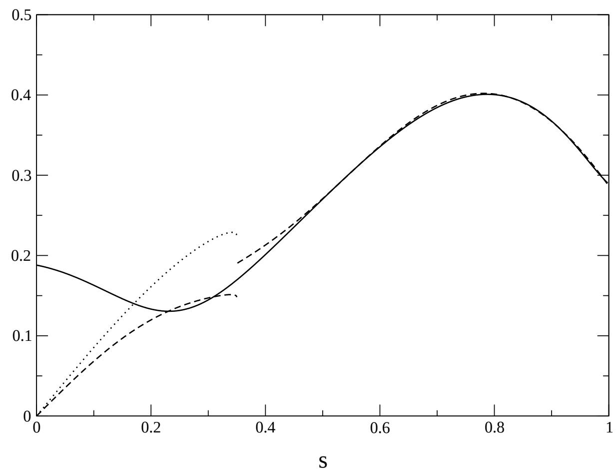

Figure 1: Cylindrical average $\{B_s^2\}^{1/2}$ in mT units respectively for the three-dimensional quasi-static magnetic field of Section 2 (full curve) and the axisymmetrical field of Section 4 (dashed curve). In the latter case, and for $s \leq b$, the dashed and dotted curves show respectively $\{B_s^2\}^{1/2}$ in the Northern and Southern Hemispheres.

the models of Zatman and Bloxham [1998] and Buffett [1998]. At $t = 0$, we set $\tau = 0$ and $\mathbf{b_m} = 0$. Finally, we make a variety of choices for the initial value of ω_g. We use conservation of total energy, kinetic and magnetic as a diagnostic, when the mantle is electrically insulating. Indeed, the last portions of our runs have to be discarded as waves with ever decreasing length-scales pile up near the rotation axis. Before this final stage, there is amplification of the motions in the equatorial region, as expected. Neither positive nor negative s-direction of propagation is favoured. We find very similar results whether we include the last surface term of Eq.(6) or not. Finally, we do not dwell on the most conspicuous feature, which is the magnification of the waves as they get nearer to the axis since it is drastically modified in presence of a solid and electrically conducting inner core.

3 Topographical effects at the CMB

It is estimated from nutation models and nutation series derived from very long baseline interferometry that the ellipticity of the fluid outer core exceeds its hydrostatic equilibrium value by 3.8% [Mathews et al., 2002]. That corresponds to an excess of the equatorial radius by $350\,m$. This value gives us a lower estimate of the height of the corrugations at the CMB. Many seismological studies have been devoted to the estimation of the CMB topography amplitude. Recently, Garcia and Souriau [2000] concluded that when averaging over regions of 20 degrees lateral extent, the topography amplitude is in the range $\sim \pm 1.5$

km. They found also larger amplitude when averaging over smaller regions. Sze and Van der Hilst [2003] concurred but argued that the currently available seismic data can resolve CMB topography at least in some regions. They found 3 km peak-to-peak undulations.

In presence of topography at the CMB or at the Inner Core Boundary (ICB), geostrophic contours deviate from circles. Then, both the magnetic and buoyancy forces contribute to the geostrophic acceleration because the component of the buoyancy force parallel to the geostrophic contours does not vanish. Propagation of torsional waves comes with a pressure torque acting at the CMB. This net torque acting on the mantle is non zero and may play a role in the changes of the Earth's rate of rotation over $10-10^2$ years. This is what motivated the inclusion of CMB topography in models of torsional waves propagation [Buffett, 1998] as the origin of core-mantle coupling is not yet elucidated. Neglecting Lorentz forces at the top of the core, the non-hydrostatic pressure can be estimated at the core surface from secular variation data [Chulliat and Hulot, 2000]. It is of the order of $\pm 10^3 Pa.$ peak-to-peak. Then, a typical magnitude of the pressure torque acting at the CMB of area Σ on the solid mantle is $hp\Sigma$ ($10^{20} N.m.$), which is 10^2 larger than the actual torque between core and mantle inferred from LOD variations. On the other hand, the typical pressure B^2/μ_0 associated with magnetic fields like the one considered in the previous section is only 0.1 Pa. More important pressures are obtained when one assumes that there is a large zonal toroidal magnetic field $B_\phi(s,z)\mathbf{e}_\phi$in the core interior, which is invisible at the core surface and is parallel to the geostrophic cylinders in spherical geometry. However, Anufriyev and Braginsky [1977] found that the magnitude of the pressure torque scales then only as $h^2 B_\phi^2 \Sigma/\mu_0 a$ because the action of the zonal pressure cancels out when integrated on the core surface. More general studies are needed to decide whether the magnetic field in the core interior can be strong enough to make the pressure field carried by the torsional oscillations significant for Earth rotation studies without making the Alfvèn timescale too rapid. Finally, other mechanisms, such as the transport of density anomalies by the torsional waves, can also be contemplated [Jault et al., 1996].

From a theoretical viewpoint, the interesting question is whether the pressure at the CMB can provide the restoring torque for differential rotation between the core and the mantle in the same way as the magnetic field provides the restoring force for torsional oscillations in the core interior. The work of Kuang and Chao (2001, 2003) gives some indication that the pressure torque may play a role of this kind. They have recently incorporated topographic coupling in a self-consistent convective dynamo model. They account for the topography by modifying the boundary conditions for the velocity and magnetic fields. That ensures that the geostrophic contours are distorted as the result of the modified no-penetration condition. They find a large cancellation in the integral that gives the pressure torque at the core surface.

A discussion of the topographical effects at the CMB starts with Eq. (3). We lump together the magnetic and buoyancy forces as a force $\mathbf{F}$. The circulation of the force $\mathbf{F}$ along a geostrophic contour $\Gamma(H,z)$ is written:

$$\oint \mathbf{F}.\mathbf{d\Gamma} = \oint F_\phi \mathbf{e}_\phi.\mathbf{d\Gamma} + \oint (F_s\mathbf{e}_s + F_z\mathbf{e}_z).\mathbf{d\Gamma} \tag{12}$$

Assuming that the corrugations are smooth and of height h small compared with the core radius a, we use a perturbation approach ($\varepsilon = h/a$). We first note that, beyond the order $O(\varepsilon)$, the interpretation of Eq. (3) as a torque balance is not correct, as already noted by Fearn and Proctor [1992] in the course of a derivation of the Taylor's condition. The angular momentum density is not uniform on the geostrophic cylinders $\mathcal{C}(H)$. The distance to the rotation axis from $\mathcal{C}(H)$ varies and the geostrophic velocity changes along a contour because the thickness of the annulus $A(H)$ enclosed between two geostrophic cylinders $\mathcal{C}(H)$ and $\mathcal{C}(H+dH)$ is not uniform. As a result, Eq. (3) cannot be transformed into a torque budget at the $O(\varepsilon^2)$ order. Eq. (3) governs the kinetic energy of the geostrophic motions rather than the angular momentum density since one way to obtain it is to take the dot product of any geostrophic-like vector field with the momentum equation. In conclusion, on the one hand, it is necessary to invoke the pressure torque to write the equation which gives the differential rotation between core and mantle but, on the other hand, it is not natural, and even not correct beyond the order $O(\varepsilon)$, to interpret the equation governing the time evolution of the geostrophic velocity as a torque budget.

Returning now to the order $O(\varepsilon)$, we would like to write how Eq. (6) is modified when the geostrophic contours are distorted. With this aim in view, it is helpful to define a spherical reference state and to transform the contours $\Gamma(H,z)$ into circles. Anufriyev and Braginsky [1977] suggested also to study separately the effects of topographies respectively symmetrical and antisymmetrical with respect to the equatorial plane. However, we are not aware that such a project has been achieved. Previous studies inspired by angular momentum considerations have included only a pressure term at the core surface to take into account topographical effects. A discussion of the symmetrical case shows that it is not satisfactory. Then, the geostrophic contours are distorted in the s-direction by an amount $\varepsilon s_1(s,\phi)$. Consider again the annulus $A(H)$ enclosed between two geostrophic cylinders $\mathcal{C}(H)$ and $\mathcal{C}(H+dH)$. There are pressure torques acting on the two interior sides $\mathcal{C}(H)$ and $\mathcal{C}(H+dH)$ of $A(H)$ and also an $O(\varepsilon)$ perturbation of the torque exerted by the force $F_\phi(s,\phi,z)\,\mathbf{e}_\phi$ on $A(H)$ because of both the variable distance to the axis along a contour and the variable thickness of $A(H)$. Thus, the action of the pressure at the top and the bottom of the annulus cannot be considered in isolation and knowing the pressure at the boundary does not suffice to calculate the influence of the boundary topography on the geostrophic acceleration.

4 Influence of a conducting inner core

In the special case of a spherical cavity enclosed between two spheres of radius respectively b and a, the geostrophic contours are circular and the geostrophic velocity is constant on each cylinder $\mathcal{C}$. However, inside the region delimited by the cylindrical surface Σ_T $(s = b)$ tangent to the inner core, the cylindrical average $\{B_s^2\}$ calculated above and below the inner core differs because the ambient magnetic field $\mathbf{B}$ is not symmetrical with respect to the equatorial plane. In the Northern and Southern hemispheres, we have respectively

$$\{B_s^2\}^+(s) = \frac{1}{2\pi H}\int_{z_B}^{z_T}\oint B_s^2 d\phi dz, \text{ and } \{B_s^2\}^-(s) = \frac{1}{2\pi H}\int_{-z_T}^{-z_B}\oint B_s^2 d\phi dz, \tag{13}$$

with $z_T = \sqrt{a^2 - s^2}$, $z_B = \sqrt{b^2 - s^2}$, and $H = z_T - z_B$. As a result, the geostrophic velocity splits up also:

$$\omega_g = \omega_g^{\pm}(s)\mathbf{e}_\phi \qquad \text{at} \quad s \leq b \quad \text{and} \quad \pm z \geq 0\,. \tag{14}$$

There is first a weak singularity at $(s = b^-)$ because the height of the geostrophic cylinder $(z_T - z_B)$ changes rapidly as s approaches b from below. However, the main singularity arises because Eq. (3) changes from one side to the other side of Σ_T. A discontinuity in the geostrophic velocity at Σ_T cannot be ruled out because viscosity is neglected in the fluid interior. Then, electrical currents set up at the cylinder Σ_T tangent to the inner core (and at the boundary with the electrically conducting inner core as well)

$$\eta\left(\frac{\partial b_\phi}{\partial s}\,|_{s=b^+} - \frac{\partial b_\phi}{\partial s}\,|_{s=b^-}\right) = -b(\omega_g(b^+) - \omega_g(b^-))B_s\,, \tag{15}$$

$$\eta\left(\frac{\partial b_\phi}{\partial r}\,|_{r=b^+} - \frac{\partial b_\phi}{\partial r}\,|_{r=b^-}\right) = -s(\omega_g(s) - \omega_{IC})B_r\,, \tag{16}$$

where ω_{IC} is the inner core rotation, and $\eta = 1/\mu_0\sigma$ is magnetic diffusivity. The equation (16) is written assuming equal conductivity σ for the solid and liquid parts of our core model.

The treatment of the inner core in previous studies was quite different from ours as equatorial symmetry was assumed. Braginsky [1970] argued that the magnetic coupling between the solid and fluid cores is so strong that $\omega_g(s) = \omega_{IC}$ for $(s \leq b)$. He solved Eq. (6) only for $(s \geq b)$ with the boundary condition $\omega_g(b) = \omega_{IC}$. As Zatman and Bloxham [1997] omitted the inner core in their model, they studied the propagation of torsional waves only for $(s \geq b)$ also. Finally, Buffett [1998] imposed the continuity of ω_g through $s = b$ and solved an equation analogous to (6) separately for $(s < b)$ and $(s > b)$ whilst Mound and Buffett [2003] assumed that, within Σ_T, ω_g is uniform but not identical to ω_{IC}. The latter authors estimated the evolution of $\omega_g(b)$ from the total electromagnetic torque acting on the region within Σ_T , which was inferred from $d\omega_g/ds \mid s = b^+$.

If either the inner core surface or the core-mantle boundary are not perfectly axisymmetrical, there are fluid lenses void of closed geostrophic contours in the vicinity of $s = b$ [Herrmann and Busse, 1998]. There, geostrophic motions may be replaced by Rossby waves, low frequency z-independent inertial waves. They have a natural frequency comparable to the frequency of the torsional Alfvèn waves [Jault, 2003]. Their possible role in the course of the propagation of Alfvèn waves within the Earth's core has not yet been investigated.

In order to give an illustrative example, we set again an initial value problem restricted, however, to axisymmetrical variables. We build an axisymmetrical model such that its distribution of $\{B_s^2\}^{1/2}$(Fig. 1, dashed curve) resembles that calculated in Section 2 from a model of the geomagnetic field at the core surface (Fig. 1, full curve) outside Σ_T. For ($s \leq b$), $\{B_s^2\}^+$in the Northern Hemisphere differs from $\{B_s^2\}^-$in the Southern Hemisphere. We assume a model for the geostrophic velocity ω_g at $t = 0$. A zonal toroidal magnetic field b_ϕ is induced. In order to study the evolution of the two scalar variables ω_g and b_ϕ, we use a finite difference code with both spherical and cylindrical grids. The two grids coincide on Σ_T so that Eq.(15) can be easily enforced [Jault, 1996]. We calculate separately ω_g at $s = b^-$and $s = b^+$. In addition, for $s < b$, the geostrophic angular velocity $\omega_g^\pm$ can differ below and above the inner core. Finally, we reinstate magnetic diffusion because, in the vicinity of the tangent cylinder Σ_T and of the inner core surface, the large gradients of b_ϕ make it important.

We have studied a few initial states for the geostrophic velocity. The ratio between the Alfvèn wave period and the magnetic dissipation time of the solid inner core depends on the magnetic Ekman number $E_M = \eta/\Omega a^2$, on the cylindrical average $\{B_s^2\}^+(s)$ and $\{B_s^2\}^-(s)$ for ($s \leq b$) and on the spherical average $(\int\int_{r=b} B_r^2 d\Sigma)/\Sigma_b$ of the radial magnetic field at the inner-core boundary of area Σ_b. The value of $((\int\int_{r=b} B_r^2 d\Sigma)/\Sigma_b)^{1/2}$ for our model of quasi-static magnetic field (0.4 mT) is similar to $\{B_s^2\}^{1/2}$. We have investigated a range of values of E_M down to 10^{-9}, which is the geophysically relevant value according to the conductivity estimates of Secco and Schloessin [1989]. We have chosen three different epochs (respectively $t = 6.7$ yr, $t = 14.3$ yr, and $t = 17.7$ yr) to illustrate the propagation of torsional waves in presence of an inner core (Fig. 2). We find that the discontinuities in ω_g at Σ_T are kept small by the Lorentz force coupling the geostrophic cylinders across Σ_T. In our example, the latter are much more efficient in the Southern Hemisphere because $(\{B_s^2\}^+(b) < \{B_s^2\}^-(b))$. After a short transient period, the torsional waves mainly propagate inwards. We attribute that to magnetic dissipation within the inner core. The waves penetrate within the tangent cylinder and are damped on a distance comparable to the inner core radius. However, the coupling between the solid inner core and the geostrophic motions remains strong in our model. There are large oscillations of the inner core, which are apparent in the time evolution of the geostrophic motions within Σ_T .

5 Concluding remarks

We have argued that a preferred direction of propagation, as observed by Hide et al. [2000] is potentially a useful constraint on the dissipation of the torsional waves, especially at the inner core boundary. We have attempted a forward modelling of the torsional Alfvèn waves without the often made assumption

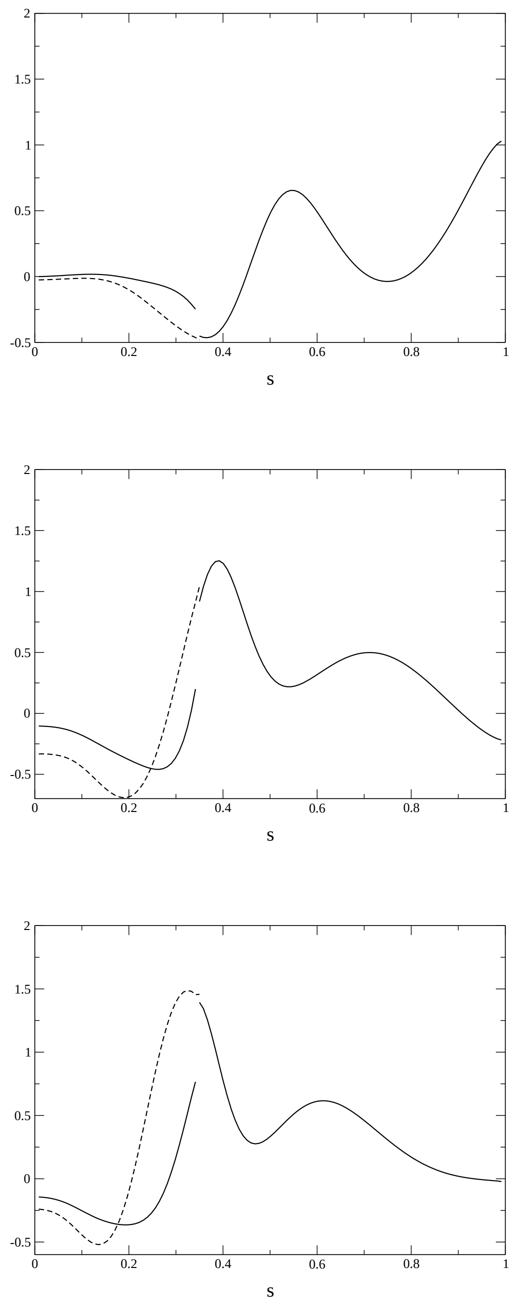

Figure 2: Snapshots of the geostrophic angular velocity at $t = 6.7$ yr (top figure), $t = 14.3$ yr (middle figure) and $t = 17.7$ yr (bottom figure). For $s \leq b$, the full and dashed curves show respectively the geostrophic velocity in the Northern and Southern Hemisphere. $Ro = 3.10^{-8}$.

that they can be represented as standing oscillations. We have been able to point up sharp velocity gradients at the cylinder Σ_T tangent to the inner core as we have not assumed equatorial symmetry of $\mathbf{B}$ in our study of the role of the inner core. We intend now to undertake an inverse modelling. In order to recover possible sharp velocity gradients at Σ_T, we will determine directly the torsional oscillations in the Earth's fluid core from geomagnetic data. Bypassing the construction of surface flow models is indeed helpful as small scale features, such as large gradients in a narrow zone, cannot be recovered from the calculation of general core surface flows. Hopefully, the recording of large geomagnetic data sets by the Ørsted, Champ, and following satellites will promote yet other theoretical progresses.

Modeling Earth's nutation, Mathews et al. [2002] estimated that the rms radial magnetic field at the ICB is 7.2 mT. This finding, which required several hypothesis, does not agree well with the models of the magnetic field in the core interior that we have used. It raises a question that we have already touched in the section on topographic effets. In our models, the strength of the magnetic field is comparable at the core surface and in the interior whereas we would have expected it to be larger in the interior from considerations on the speed of core motions.

We have just sketched a discussion of topographic coupling. We especially expect from a study of torsional waves propagation in a core model including corrugated boundaries to learn whether pressure effects tend to restore corotation between core and mantle or whether other mechanisms (viscous, electromagnetic) have to be taken into account at the CMB.

Acknowledgements

This contribution is dedicated to the memory of Stephen Zatman who, together with Professor Jeremy Bloxham, rejuvenated the study of torsional Alfvén waves inside the Earth's core before his untimely death.

DJ thanks gratefully Professor Fritz Busse who suggested that torsional waves arriving at the tangent cylinder or at the CMB equator may cause sudden changes in the geomagnetic field.

References

M. Alexandrescu, D. Gibert, G. Hulot, J.-L. Le Mouël, and Saracco G. Worldwide wavelet analysis of geomagnetic jerks. *J. Geophys. Res.*, 101:21975–21994, 1996.

A. P. Anufriyev and S. I. Braginsky. Effects of irregularities of the boundary of the Earth's core on the speed of the fluid and on the magnetic field. iii. *Geomag. Aeron.*, 17:492–496, 1977.

P. I. Bell and A. M. Soward. The influence of surface topography on rotating convection. *J. Fluid Mech.*, 313:147–180, 1996.

J. Bloxham, S. Zatman, and M. Dumberry. The origin of geomagnetic jerks. *Nature*, 420:65–68, 2002.

S. I. Braginsky. Torsional magnetohydrodynamic vibrations in the Earth's core and variations in day length. *Geomag. Aeron.*, 10:1–8, 1970.

B. A. Buffett. Free oscillations in the length of day: inferences on physical properties near the core-mantle boundary. In M. Gurnis, M. E. Wysession, E. Knittle, and Buffett B. A., editors, *The Core-Mantle Boundary Region*, volume 28 of *Geodynamics Series*, pages 153–165. AGU, 1998.

A. Chulliat and G. Hulot. Local computation of the geostrophic pressure at the top of the core. *Phys. Earth Planet. Inter.*, 117:309–328, 2000.

J. Ducruix, V. Courtillot, and J.-L. Le Mouël. The late 1960s secular variation impulse, the eleven year magnetic variation and the electrical conductivity of the deep mantle. *Geophys. J. R. Astr. Soc.*, 61:73–94, 1980.

S. Duhau and E. A. Martinez. On the origin of the fluctuations in the length of day and in the geomagnetic field on a decadal time scale. *Geophys. Res. Lett.*, 22:3283–3286, 1995.

D. R. Fearn and M. R. E. Proctor. Magnetostrophic balance in non-axisymmetric, non-standard dynamo models. *Geophys. Astrophys. Fluid Dyn.*, 67:117–128, 1992.

R. Garcia and A. Souriau. Amplitude of the core-mantle boundary topography estimated by stochastic analyses of core phases. *Phys. Earth Planet. Inter.*, 117:345–359, 2000.

J. Herrmann and F. H. Busse. Stationary and time dependent convection in the rotating cylindrical annulus with modulated height. *Phys. Fluids*, 10: 1611–1620, 1998.

R. Hide, D. H. Boggs, and Dickey J. O. Angular momentum fluctuations within the Earth's liquid core and torsional oscillations of the core-mantle system. *Geophys. J. Int.*, 143:777–786, 2000.

G. Hulot, C. Eymin, B. Langlais, M. Mandea, and N. Olsen. Small-scale structure of the geodynamo inferred from Oersted and Magsat satellite data. *Nature*, 416:620–623, 2002.

A. Jackson, J. Bloxham, and D. Gubbins. Time-dependent flow at the core surface and conservation of angular momentum in the coupled core-mantle system. In J.L. Le Mouël, D.E. Smylie, and T. Herring, editors, *Dynamics of the Earth's Deep Interior and Earth Rotation*, pages 97–107. AGU/IUGG, 1993.

D. Jault. Sur l'inhibition de la régénération du champ magnétique dans certains modèles de dynamo planétaire en présence d'une graine solide. *C.R.Acad. Sci. Paris, série II a*, 323:451–458, 1996.

D. Jault. Electromagnetic and topographic coupling, and LOD variations. In C. A. Jones, A. M. Soward, and K. Zhang, editors, *Earth's Core and Lower Mantle*, The Fluid Mechanics of Geophysics and Astrophysics, pages 56–76. Taylor and Francis, 2003.

D. Jault, C. Gire, and J.-L. Le Mouël. Westward drift, core motions and exchanges of angular momentum between core and mantle. *Nature*, 333:353–356, 1988.

D. Jault, G. Hulot, and J.-L. Le Mouël. Mechanical core-mantle coupling and dynamo modelling. *Phys. Earth Planet. Inter.*, 43:187–191, 1996.

A. R. T. Jonkers, A. Jackson, and A. Murray. Four centuries of geomagnetic data from historical records. *Rev. Geophys.*, 41 (1006):10.1029/2002RG000115, 2003.

W. Kuang and B. F. Chao. Topographic core-mantle coupling in geodynamo modeling. *Geophys. Res. Lett.*, 28:1871–1874, 2001.

W. Kuang and B. F. Chao. Geodynamo modeling and core-mantle interactions. In V. Dehant, K. C. Creager, S.-I. Karato, and S. Zatman, editors, *Earth's Core Dynamics, Structure, Rotation*, Geodynamics Series, pages 193–212. AGU, 2003.

S. R. C. Malin and B. M. Hodder. Was the 1970 geomagnetic jerk of internal origin? *Nature*, 296:726–728, 1982.

P. M. Mathews, T. A. Herring, and B. A. Buffett. Modeling of nutation-precession: New nutation series for nonrigid Earth, and insights into the Earth's interior. *J. Geophys. Res.*, 107(B4):doi:10.1029/2001JB000390, 2002.

J. E. Mound and B. A. Buffett. Interannual oscillations in length of day: Implications for the structure of the mantle and core. *J. Geophys. Res.*, 108 (B7): 10.1029/2002JB002054, 2003.

N. Olsen. A model of the geomagnetic field and its secular variation for epoch 2000 estimated from Ørsted data. *Geophys. J. Int.*, 149:454–462, 2002.

A. Pais and G. Hulot. Length of day decade variations, torsional oscillations and inner core superrotation: evidence from recovered core surface zonal flows. *Phys. Earth Planet. Inter.*, 118:291–316, 2000.

P. H. Roberts. *An introduction to magnetohydrodynamics*. Elsevier, New York, 1967.

R.A. Secco and H.H. Schloessin. The electrical resistivity of solid and liquid Fe at pressures up to 7 GPa. *J. Geophys. Res.*, 94:5887–5894, 1989.

E. K. M. Sze and R. D. Van der Hilst. Core mantle boundary topography from short period PcP, PKP, and PKKP data. *Phys. Earth Planet. Inter.*, 135: 27–46, 2003.

S. Zatman and J. Bloxham. Torsional oscillations and the magnetic field within the Earth's core. *Nature*, 388:760–763, 1997.

S. Zatman and J. Bloxham. A one-dimensional map of B_s from torsional oscillations of the Earth's core. In M. Gurnis, M. E. Wysession, E. Knittle, and Buffett B. A., editors, *The Core-Mantle Boundary Region*, volume 28 of *Geodynamics Series*, pages 183–196. AGU, 1998.